

# The quasinormal modes of Reissner-Nordström black holes

Edward W. Leaver

Jet Propulsion Laboratory

California Institute of Technology

4800 Oak Grove Drive

Pasadena, CA 91109

## Abstract

We present a matrix-eigenvalue algorithm for accurately computing the quasinormal frequencies and modes of charged static black holes. The method is then refined through the introduction of a continued fraction step. We believe the approach will generalize to a variety of non-separable wave equations, including the Kerr-Newman case of charged rotating black holes.

## 1 Introduction

The dynamic perturbations of uncharged rotating and static charged black holes are described by one of several separable second order linear partial differential equations. For Schwarzschild black holes these are the Regge-Wheeler<sup>[1]</sup> and Zerilli<sup>[2]</sup> equations, and for Kerr black holes the Teukolsky<sup>[3]</sup> equations. The perturbation equations for the charged Reissner-Nordström black hole were also derived by Zerilli,<sup>[4]</sup> and by Moncrief.<sup>[5]</sup> The theory of dynamic black hole perturbations and their associated quasinormal resonances is discussed in references [6, 7, 8, 9], and [10]. Stationary perturbations of Reissner-Nordström black holes are discussed by Dvořák.<sup>[11]</sup> A fundamental difficulty in quantitatively characterizing black hole resonances is that the numerical solutions of these differential equations are unstable in the frequency region of interest.<sup>[12]</sup> Chandrasekhar and Detweiler<sup>[7]</sup> developed a numerical procedure that reduced (but did not eliminate) this instability, and were able to integrate the Regge-Wheeler equation with accuracy sufficient to compute the fundamental quasinormal frequencies, and the first overtones, for each multipole moment for the Schwarzschild black hole. The method was successfully applied to the uncharged rotating Kerr black hole by Detweiler,<sup>[13]</sup> and to the charged static Reissner-Nordström black hole by Gunter.<sup>[9]</sup>

Implicit in the Chandrasekhar–Detweiler scheme was the understanding that for each multipole the number of underdamped modes was (approximately) equal to the multipole index  $l$ . Although an infinity of undamped modes for a very rapidly rotating hole was demonstrated by Detweiler,<sup>[13]</sup> the question of whether there were more Schwarzschild modes, presumed to be overdamped, remained open<sup>[14]</sup> until a stable continued fraction method for computing them was discovered.<sup>[15]</sup> This method allowed connection to be made between certain overdamped Schwarzschild modes and Detweiler’s undamped modes at the Kerr limit. The contribution of individual modes to particular physical Schwarzschild gravitational waveforms, with concomitant emphasis on computing the quasinormal mode wavefunctions as well as the frequencies, was demonstrated shortly thereafter.<sup>[16]</sup>

Significant semi-analytic contributions to black hole normal mode analysis have been pioneered by Mashhoon<sup>[17]</sup> and by Schutz and Will,<sup>[18]</sup> and their coworkers.<sup>[19, 20]</sup> Indeed, the suggestion of the existence of an infinity of overdamped modes is implicit in the work of Ferrari and Mashhoon,<sup>[21]</sup> and the present study was itself prompted by a recent higher-order WKB analysis of Reissner-Nordström quasinormal frequencies. In that article,<sup>[22]</sup> Kokkotas and Schutz raise the interesting question of whether the continued fraction method employed previously by us

to determine the quasinormal frequencies and modes of uncharged black holes is applicable to the Reissner-Nordström case. We show here that – with suitable generalization – it is.

## 2 Recurrence Relations

As mentioned previously, an early difficulty in characterizing the quasinormal modes of uncharged black holes was the numerical instability of the radial components of the Regge-Wheeler and Teukolsky equations in the frequency regions of interest. The motivation behind our previous work was to transform these unstable ordinary differential equations into stable algebraic recurrence relations, and to exploit the analytic and numeric properties of the recurrence relations to find the quasinormal frequencies and generate their corresponding modes. In the particular case studied, that of the uncharged Kerr black hole, the resulting recurrence relations were of the three-term variety and hence amenable to relatively elegant continued fraction solutions. However, the basic method is not necessarily limited to recurrence relations of this type. Indeed, if one follows the sequence of linear second order one dimensional wave equations, one finds that wave equations with one coordinate singularity, such as Bessel equations and the Coulomb wave equation, possess one regular singular point and one irregular (confluent) singular point at spatial infinity. Their series solutions are the well-known confluent hypergeometric series and are characterized by two-term recurrence relations connecting the expansion coefficients.<sup>[23]</sup> Likewise, the spheroidal wave equations (of which the Regge-Wheeler and Teukolsky equations are special cases) possess, in addition to the obligatory confluent singularity, *two* regular singular points corresponding to the two foci of the spheroidal coordinates.<sup>[24]</sup> And the series representations of the spheroidal wavefunctions have three-term recurrence relations connecting their coefficients.<sup>[25, 26, 27, 28]</sup> (Three-term recurrence power series solutions to the Regge-Wheeler equation were first formulated by Arenstorf, Cohen, Kearney, and Kegeles,<sup>[29]</sup> although the form these authors used is not, and was not intended to be, suitable for quasinormal mode calculations. Earlier analytic contributions were made by Persides.<sup>[30]</sup>)

One then might speculate whether the Zerilli-Moncreif equation which describes odd-parity perturbations of the static charged black hole, being a wave equation with a confluent singularity and *three* regular singular points (making it an ellipsoidal wave equation<sup>[31]</sup>), possesses series solutions whose coefficients are connected by *four*-term recurrence relations. To confirm this conjecture we first scale the radial coordinate, frequency parameter, and charge by the mass  $M$  of the black hole:  $r \rightarrow r/2M$ ,  $\rho = -2Mi\omega$ , and  $Q = Q_*/2M$ ,  $0 \leq Q < 1/2$  in these units. Assume an  $\exp \rho t$  time dependence. Then, following Moncrief,<sup>[5]</sup> Chandrasekhar<sup>[32]</sup> and Gunter,<sup>[9]</sup> write the odd parity equation for multipole index  $l$  as

$$\left[ \frac{d^2}{dr_*^2} - \rho^2 - V_i^{(-)}(r) \right] Z_i^{(-)}(r) = 0 \quad (1)$$

where

$$\begin{aligned} \frac{dr}{dr_*} &= \frac{\Delta}{r^2}, \\ \Delta &= r^2 - r + Q^2 \equiv (r - r_-)(r - r_+), \\ V_i^{(-)}(r) &= \frac{\Delta}{r^5} (Ar - q_j + 4Q^2/r), \\ A &= l(l+1), \\ q_1 &= \left( 3 + \sqrt{9 + 16Q^2(l-1)(l+2)} \right) / 2, \\ q_2 &= \left( 3 - \sqrt{9 + 16Q^2(l-1)(l+2)} \right) / 2, \\ \text{and } i, j &= 1, 2 \ (i \neq j). \end{aligned}$$

The functions  $Z_1^{(-)}$  and  $Z_2^{(-)}$  correspond to those odd parity perturbations that are respectively purely electromagnetic and purely gravitational at the Schwarzschild limit ( $Q = 0$ ). Even parity perturbations are obtained from the odd parity solutions via the transformation<sup>[33]</sup>

$$[A(A-2) - \rho q_j] Z_i^{(+)} = \left[ A(A-2) + \frac{2q_j^2 \Delta}{r^3[(A-2)r + q_j]} \right] Z_i^{(-)} + 2q_j \frac{dZ_i^{(-)}}{dr_*}. \quad (2)$$

The confluent singular point of equation (1) is at  $r = \infty$ , and the three regular singular points are at  $r = 0$  and at the inner (Cauchy) and outer (event) horizons,  $r_{\pm} \equiv (1 \pm \sqrt{1 - 4Q^2})/2$ . Making a Jaffé-Baber-Hassé transformation<sup>[34, 35, 15]</sup> of the independent variable, incorporating boundary conditions appropriate for quasinormal modes,<sup>[32, 9, 22]</sup> and applying a bit of algebra, we obtain the (suitably normalized) form

$$Z_i^{(-)} = r_+ e^{2\rho r_+} (r_+ - r_-)^{2\rho-1} [r^{-1} (r - r_-)^{1-\rho} e^{-\rho r}] u^b \sum_{n=0}^{\infty} a_n u^n, \quad (3)$$

where  $u \equiv (r - r_+)/ (r - r_-)$  and the exponent  $b = \rho r_+^2 / (r_+ - r_-)$  is the solution to the indicial equation at  $r = r_+$  that corresponds to ingoing wave behavior at the outer ( $r_+$ ) horizon. The sum of the exponents of  $r$ ,  $(r - r_-)$ , and  $(r - r_+)$  is determined by the outgoing condition at spatial infinity:  $\lim_{r \rightarrow \infty} Z_i^{(-)} \propto \exp -\rho(r + \ln r)$ . The particular exponents for  $r$  and  $(r - r_-)$  are then determined by the requirement that the recursion relation be as simple as possible, in this case four terms. The normalization chosen is that used by Gunter and by Kokkotas and Schutz, *vis*

$$\lim_{r_* \rightarrow -\infty} Z_i^{(-)} = e^{\rho r_*}, \quad (4)$$

where the tortoise coordinate  $r_*$  is given by

$$r_* = \int \frac{r^2}{\Delta} dr = r + \frac{r_+^2}{r_+ - r_-} \ln(r - r_+) - \frac{r_-^2}{r_+ - r_-} \ln(r - r_-), \quad (5)$$

so that with the series normalized to  $a_0 = 1$  we have

$$\lim_{r_* \rightarrow -\infty} Z_i^{(-)} = e^{\rho r_+} (r_+ - r_-)^{-\rho r_+^2 / (r_+ - r_-)} (r - r_+)^b, \quad (6)$$

and

$$\lim_{r_* \rightarrow +\infty} Z_i^{(-)} = \left[ r_+ e^{2\rho r_+} (r_+ - r_-)^{2\rho-1} \sum_{n=0}^{\infty} a_n \right] e^{-\rho r_*}, \quad (7)$$

providing  $\sum a_n$  converges. The expansion coefficients  $a_n$  in equation (3) are then defined by

$$\begin{aligned} \alpha_0 a_1 + \beta_0 a_0 &= 0, \\ \alpha_1 a_2 + \beta_1 a_1 + \gamma_1 a_0 &= 0, \\ \alpha_n a_{n+1} + \beta_n a_n + \gamma_n a_{n-1} + \delta_n a_{n-2} &= 0, \quad n = 2, 3, \dots, \end{aligned} \quad (8)$$

where the recurrence coefficients are given in terms of the black hole parameters by

$$\begin{aligned} \alpha_n &= [n^2 + 2(b+1)n + 2b+1]r_+, \\ \beta_n &= (-2 + r_-)n^2 + [-2 - 2b(2 - r_-) - 4\rho r_+^2 + 6r_-]n \\ &\quad + [q_j - 2\rho^2 r_+^3 - 4\rho r_+^2(1+b) - 2b^2(2 - r_+^{-1}) - r_+ A - (3 - 2b)r_-], \\ \gamma_n &= (1 + r_-)n^2 + [2\rho r_+(1 + 2r_-) + 2b(1 + r_-) - 10r_-]n \\ &\quad + \{\rho r_+[2 - 12r_- + (\rho + 2b)(1 + 2r_-)] - 1 - q_j - 2b(1 + 3r_-) \\ &\quad + b^2[16 + 8r_- - (15 - 38r_- + 26r_-^2)r_+^{-3}] + (A + 13)r_-\}, \\ \delta_n &= [-n^2 + 2(3 - \rho - b)n - (9 + 4\rho b - 6b - 6\rho)]r_-. \end{aligned} \quad (9)$$

Again, the expansion coefficients are normalized so that  $a_0 = 1$ . Each of equations (9) can be scaled by a factor  $n^{-2}$  for  $n > 0$ , or by  $b^{-2}$  if  $|b| > n$ . In the Schwarzschild limit where  $Q \rightarrow 0$ ,  $r_- \rightarrow 0$ ,  $r_+ \rightarrow 1$ ,  $b \rightarrow \rho$ , equations (3) – (9) revert to the three term expression studied previously (reference [15], equations 6–8); the quasinormal frequencies were found then to be those values of the frequency parameter  $\rho$  for which the series (3) converged when  $Q$  and  $r_-$  were zero. (Note also the recurrence coefficients for the expansion of the Reissner-Nordström quasinormal modes depend on charge, through the quantity  $b$  in equation 9 above, in a way analogous to the dependence on angular momentum of the recurrence coefficients for the expansion of the Kerr quasinormal modes, equation (26) of reference [15].) The next question becomes whether the corresponding convergent solution to the four-term recurrence relation (8) is also numerically stable in the presence of charge, and if so, how to find it.

[As an aside, it is important to note the singularity rearrangement effected by the change of independent variable from  $r$  to  $u$ . The regular singularity at  $r = r_+$  is at  $u = 0$ , the confluent singularity at  $r = \infty$  appears at  $u = 1$ , and the regular singularities at  $r = 0$  and  $r = r_-$  appear respectively at  $u = r_+/r_-$  and at  $u = -(r_+ - r_-)\infty$ . Clearly the power series expansion in  $u$  is useless at the limit of maximal charge when  $r_- = r_+$  and  $u \equiv 1$ . It is therefore a mistake to read more analytic information into the leading factors of expansion (3) than is actually present: their apparently singular behavior at maximal  $Q$  will later be seen to be exactly cancelled by equally singular behavior of the series  $\sum a_n u^n$ . However the maximal  $Q$  limit is not physically realizable, and we return to the  $Q < 1/2$  case.]

### 3 The Solution

We discuss two equivalent approaches, the second of which may be considered a refinement of the first. Equations (8) define an infinite banded matrix equation of width four which in the Schwarzschild limit reduces to an infinite tridiagonal system. The clue to its solution is (again) to be found in studies of the one-particle Schrödinger equation with two-center Coulomb potential. From an article by M. Shimizu:

“The eigenvalue equation is equivalent to an  $\infty$ -dimensional secular equation. A way to solve it is to approximate the  $\infty$ -dimensional matrix by a finite one of an appropriate order. Then the calculation can be made quite straightforwardly... The actual calculations are carried out for a seven dimensional matrix. Within the accuracy required, these solutions coincide completely with those obtained by using a nine dimensional matrix as long as the dipole moment is not large. As a check of these calculations, the continued fraction method and the expansion of the determinant of the secular equation by an adequate series of its non-diagonal elements are also employed. . .”<sup>[36]</sup>

This connection is not new; the intimate relationship between continued fractions and the determinants of truncated tridiagonal systems was exploited as early as sixty years ago.<sup>[25]</sup> We explicitly chose the continued fraction method in our investigations of uncharged black holes because the inversion properties of continued fractions allow stable and accurate determination of the higher order eigenfrequencies.<sup>[37]</sup> Comparison with previously computed low-lying black hole resonances<sup>[7, 13]</sup> allowed us to confirm the validity of our derivations at the fundamental quasinormal frequency and the first overtone. Repeated inversion of the continued fractions then lead to the (more-or-less) complete characterization of the quasinormal mode spectrum of the Kerr black hole.



determine  $a_{N-1}$  from  $a_{N-1} = -a_N \beta_N / \gamma_N$ , and generate the remainder of the  $a_n$  by downward recursion. In our case the frequency would be an eigenfrequency, and the minimal solution vector an eigenvector, if the first of equations (8) were then satisfied. The value of  $N$  is then increased until the normalized values of the desired small  $n$  terms, and the corresponding eigenvalues, no longer appreciably change. This procedure (and the eigenvalue condition) is specified exactly by the truncated tridiagonal matrix equation (10), in the Schwarzschild limit when the  $\delta_n$  are zero.<sup>[41]</sup>

The important point is that generation of the minimal solution vector is numerically stable only under downward recursion from large  $n$ , and it is possible to do this only when the matrix is upper-triangular or (as a special case) tridiagonal. Therefore when  $Q \neq 0$  the  $\delta_n$  must be eliminated from the singular matrix obtained upon completing the root search before the eigenvector can be generated. This Gaussian-type elimination step involves only a straightforward (and in this case stable) upward recursion from the  $n = 1$  equation and, aside from an overall normalization, completes our first method of solution. But it is this last consideration of the generation of the eigenvector that suggests a simplification that can ease considerably the automatic generation of Reissner-Nordström quasinormal frequencies and modes.

## 4 Refinement of the Solution

The matrix-determinant algorithm just presented, while simple to implement, lacks somewhat in robustness. There are two reasons. First, given the known nature of the solution sequences  $\{a_n\}$  in the Schwarzschild limit as a function of the overtone index  $q = 0, 1, 2, \dots$ , namely that the  $a_n$  increase rapidly with  $n$  for  $n$  less than the overtone index  $q$ , and that convergence does not set in until after  $n$  becomes greater than this value,<sup>[42]</sup> we can expect the matrix order  $N$  required to accurately approximate the quasinormal frequencies to be a strongly increasing function of the overtone index. Second, due to the confluence of the two horizons as the charge parameter approaches its limiting value  $Q = 1/2$ , the required matrix order is also a function of  $Q$ . Thus there is no *a priori* way of knowing the matrix order needed to yield a given accuracy of the quasinormal eigenfrequency, even for a fixed overtone, and much redundant computation on ever increasing values of  $N$  is required to obtain reliable results.

Precisely the same problems were encountered for the Kerr black hole: there the convergence of the solution sequences depended on both the overtone index and the angular momentum parameter, the latter in a way analogous to the present dependence on charge. In the Kerr case the continued fraction representation of the solutions showed its full power, for although the number of series terms necessary to represent the continued fraction increased with angular momentum, the continued fraction evaluation algorithm automatically generated just enough terms to provide a given accuracy of representation. The particular continued fraction evaluation algorithm we use is quite robust: in contrast to methods that evaluate an infinite continued fraction as an infinite sequence of rational approximants, the numerator and denominator series of which are susceptible to overflow and therefore usually require rescaling, this algorithm expresses the infinite continued fraction as an infinite series that converges if-and-only-if the fraction converges. The method is impervious to scaling problems, and its iteration loop requires but seven executable statements.<sup>[43]</sup>

Specifically, when one has prior knowledge of the convergence properties of the sequence that defines a continued fraction, as we have in equation (11), it may be permissible to sum the continued fraction's series head-to-tail, and to truncate it after the magnitudes of the successive terms have decreased to less than some specified tolerance. To justify this basis for truncation in the Schwarzschild case, note that equation (11) implies that

$$a_n \sim n^{2\rho-3/4} e^{\pm\sqrt{8\rho n}} \quad (12)$$

for large  $n$ , and that the lower (negative) sign is always obtained for the minimal sequence selected by the continued fraction. Since  $Re\rho < 0$  for quasinormal frequencies, the error introduced by truncating the series  $N$  terms after the onset of asymptotic behavior is approximately

$$E_N = \left| \int_N^\infty a_n dn \right| \sim \left| 2 \int_{\sqrt{N}}^\infty z^{4\rho-1/2} e^{-\sqrt{8\rho}z} dz \right|, \quad (13)$$

The exponential term guarantees adequate convergence of the integral near the lower quasinormal overtone frequencies where  $|Im\rho| > |Re\rho|$  and  $|\rho| \sim 1$ , while the  $z^{4\rho-1/2}$  term assures somewhat slower convergence as the overtone index increases. Hence

$$E_N < \min \left( \left| \frac{N^{2\rho-1/4}}{2\rho-1/4} \right|, \left| \frac{e^{-\sqrt{8\rho}N}}{\sqrt{2\rho}} \right| \right), \quad (14)$$

and we have a simple method of determining an upper bound on the number of terms  $N_E$  necessary to retain if the series is to be truncated with error less than  $E \ll 1$  at the Schwarzschild limit:

$$N_E \geq \max \left( \left| [(2\rho-1/4)E]^{1/(2\rho-1/4)} \right|, \left| [\ln(\sqrt{2\rho}E)]^2 / (8\rho) \right| \right). \quad (15)$$

The error estimates (14) and (15) tend to considerably overestimate the actual truncation error since the  $\exp \sqrt{8\rho n}$  in (12) make the  $a_n$  an alternating series, albeit with a period proportional to  $\sqrt{n}$ . While a rigorous analysis of the behavior of such series is possible, in practice one empirically observes that if the series in the continued fraction algorithm is terminated after the relative magnitude of each successive term becomes smaller than  $10^{-d}$  (where there are  $d$  digits of desired accuracy), then subsequent inclusion of more terms in the series only effects the relative value of the quasinormal frequency being evaluated by approximately this amount. Therein lies the elegance of the method: the continued fraction algorithm automatically retains just the number of terms sufficient to produce a specified accuracy.

One is not so fortunate when dealing with the truncated matrix equation (10) of the previous section. There the truncation order  $N$  was determined by comparing the quasinormal frequency values obtained from employing successively larger orders, and halting when the differences became acceptably small. In the Schwarzschild limit one finds (not surprisingly) that the order of the matrix needed to produce a given accuracy is precisely the number of terms that the continued fraction algorithm retains automatically. What is desired is a method to incorporate this feature of continued fraction evaluation when the charge  $Q$  and the  $\delta_n$  in equation (10) are not zero.

We do this by inserting a Gaussian elimination step into our quasinormal frequency algorithm. For each value of  $\rho$  used in the root search we first tridiagonalizing matrix equation (10), then realize that the quasinormal frequency search is for those values of  $\rho$  for which the determinant is *zero*, which are precisely those values of  $\rho$  for which the tridiagonal matrix problem possesses minimal solution vectors and hence zero the continued fraction, expression (19) below. The zeroes of the determinant (tridiagonalized or not) and of the continued fraction are identical.<sup>[44]</sup>

The elimination step acts recursively on each row starting from the top ( $n = 2$ ), so it too need be used only on the number of rows necessary for the fraction to converge. The method is equivalent to the one presented in the previous section, and again we find that the number of terms selected by the continued fraction algorithm to produce quasinormal frequency values of a desired accuracy is identical to the order  $N$  needed to produce the same accuracy directly from equation (10). The advantage here is that the continued fraction method does not require the value of  $N$  in advance, nor does it require storage for a large matrix. And the inversion properties of the continued fraction allow the stable computation of the higher quasinormal overtones. Explicitly, the transformed recurrence relation is

$$\begin{aligned} \alpha'_0 a_1 + \beta'_0 a_0 &= 0, \\ \alpha'_n a_{n+1} + \beta'_n a_n + \gamma'_n a_{n-1} &= 0, \quad n = 1, 2, \dots, \end{aligned} \quad (16)$$

where the recurrence coefficients are given in terms of the  $\alpha_n$ ,  $\beta_n$ ,  $\gamma_n$  and  $\delta_n$  of equation (9) by

$$\begin{aligned} \alpha'_n &= \alpha_n, \quad \beta'_n = \beta_n, \quad \gamma'_n = \gamma_n \quad \text{for } n = 0, 1 \\ \text{and} \\ \delta'_n &\equiv 0, \\ \alpha'_n &\equiv \alpha_n, \\ \beta'_n &= \beta_n - \alpha'_{n-1} \delta_n / \gamma'_{n-1}, \\ \gamma'_n &= \gamma_n - \beta'_{n-1} \delta_n / \gamma'_{n-1}, \quad \text{for } n \geq 2. \end{aligned} \quad (17)$$

The ratios of successive terms of the solution eigenvector  $\{a_n : n = 0, 1, 2, \dots\}$  is given by the continued fraction

$$\frac{a_{n+1}}{a_n} = - \frac{\gamma'_{n+1}}{\beta'_{n+1} - \frac{\alpha'_{n+1} \gamma'_{n+2}}{\beta'_{n+2} - \frac{\alpha'_{n+2} \gamma'_{n+3}}{\beta'_{n+3} - \dots}}} \quad (18)$$

and the quasinormal frequencies of the Reissner-Nordström black hole are then the solutions to the (implicit) characteristic continued fraction equation

$$0 = \beta'_0 - \frac{\alpha'_0 \gamma'_1}{\beta'_1} - \frac{\alpha'_1 \gamma'_2}{\beta'_2} - \frac{\alpha'_2 \gamma'_3}{\beta'_3} - \dots \quad (19)$$

or any of its inversions. As usual, the zeroes of the continued fraction are found using Minpack routine HYBRD.<sup>[45]</sup> After a quasinormal eigenfrequency is found as a solution to equation (19) the corresponding eigenvector  $\{a_n\}$  is found by first generating  $a_0$  through  $a_{q-1}$  (where  $q$  is the quasinormal overtone index,  $q = 1$  at the fundamental frequency) by forward recursion on equations (16), applying equation (18) at suitably large  $N$ , then generating the remainder of the  $a_n$  by downward recursion from this ratio and matching with the values at  $n = q - 1$ .

#### 4.1 Convergence

Surprisingly, the tridiagonalized problem (16) admits to asymptotic analysis of the solution vector  $\{a_n\}$  despite the recursive nature of the elimination step (17). Indeed, if one divides the defining equations (9) by  $n^2$  and writes the asymptotic (large  $n$ ) forms of the tridiagonalized recurrence coefficients as

$$\begin{aligned} \alpha'_n &\sim r_+(1 + u/n) \\ \beta'_n &\sim -r_+(2 + v/n) \\ \gamma'_n &\sim r_+(1 + w/n), \end{aligned} \quad (20)$$

substitutes these expressions into equations (16) and (17) and solves for  $u$ ,  $v$ , and  $w$ , one finds that

$$\begin{aligned} u &= 2(b + 1) \\ v &= 2 + 4(\rho r_+ + b) \\ w &= 2(\rho + b). \end{aligned} \quad (21)$$

The analysis involving equations (42–46) of reference [28] can then be followed to yield the desired result,

$$\lim_{n \rightarrow \infty} \frac{a_{n+1}}{a_n} \sim 1 \pm \frac{[2\rho(r_+ - r_-)]^{\frac{1}{2}}}{n^{\frac{1}{2}}} + \frac{2\rho r_+ - \frac{3}{4}}{n} + \dots \quad (22)$$

as a simple generalization of equation (11) to the case of non-zero charge. (Details are given in Appendix A.) This result confirms our intuitive guess that convergence of the series  $\sum a_n$  will become much less rapid as  $Q \rightarrow 1/2$  and  $r_- \rightarrow r_+$ , and allows an error analysis analogous to that of equations (12) – (15). However, as a practical matter this  $Q$  dependence is not a great restriction: even for  $Q$  as large as 0.49995 we find  $r_+ - r_- = \sqrt{1 - 4Q^2} \sim 0.014$ , so that a sufficient number of terms can readily be retained even for computations quite close to the limit of maximal charge.

## 5 quasinormal frequencies

Some representative Reissner-Nordström quasinormal frequencies for multipoles  $l = 1$  and  $l = 2$  are listed in table 1.

Q	$l = 2, i = 2$		$l = 2, i = 1$		Q	$l = 1, i = 1$	
n=0							
0.00	45	(-0.17792, -0.74734)	39	(-0.19001, -0.91519)	0.00	74	(-0.18498, -0.49653)
wkbj		(-0.17844, -0.74632)		(-0.19012, -0.91426)	0.10	75	(-0.18580, -0.50295)
0.20	48	(-0.17880, -0.75687)	41	(-0.19288, -0.95985)	0.20	76	(-0.18831, -0.52384)
		(-0.17928, -0.75584)		(-0.19296, -0.95896)	0.30	80	(-0.19241, -0.56551)
0.40	63	(-0.17929, -0.80243)	48	(-0.19814, -1.14026)	0.40	93	(-0.19654, -0.64699)
		(-0.17968, -0.80108)		(-0.19798, -1.13952)	0.45	98	(-0.19487, -0.72165)
0.495	146	(-0.16853, -0.85859)	92	(-0.17728, -1.38550)	0.495	150	(-0.17420, -0.84279)
		(-0.17064, -0.85660)		(-0.17834, -1.38500)	0.4975	174	(-0.17086, -0.85253)
0.4995	244	(-0.16708, -0.86227)	145	(-0.17255, -1.40620)	0.4995	228	(-0.16776, -0.86062)
0.49995	313	(-0.16729, -0.86196)	149	(-0.17241, -1.40815)	0.49995	218	(-0.16686, -0.86283)
n=1							
0.00	81	(-0.54783, -0.69342)	63	(-0.58142, -0.87308)	0.00	181	(-0.58733, -0.42903)
wkbj		(-0.54982, -0.69204)		(-0.58194, -0.87166)	0.10	176	(-0.58935, -0.43626)
0.20	84	(-0.55025, -0.70346)	65	(-0.58938, -0.92000)	0.20	175	(-0.59533, -0.45977)
		(-0.55218, -0.70196)		(-0.58968, -0.91856)	0.30	181	(-0.60450, -0.50661)
0.40	106	(-0.54989, -0.75381)	75	(-0.60212, -1.10999)	0.40	198	(-0.61070, -0.59802)
		(-0.55250, -0.75096)		(-0.60136, -1.10812)	0.45	180	(-0.59979, -0.68087)
0.495	197	(-0.51403, -0.80704)	111	(-0.53501, -1.35732)	0.495	220	(-0.52932, -0.79794)
		(-0.52868, -0.80676)		(-0.54230, -1.35788)	0.4975	241	(-0.52000, -0.80390)
0.4995	257	(-0.51030, -0.80875)	136	(-0.52144, -1.37419)	0.4995	260	(-0.51197, -0.80812)
0.49995	190	(-0.51411, -0.78618)	104	(-0.52512, -1.36630)	0.49995	98	(-0.51941, -0.81204)
n=2							
0.00	154	(-0.95655, -0.60211)	105	(-1.00318, -0.80237)	0.00	446	(-1.05038, -0.34955)
wkbj		(-0.94212, -0.60586)		(-0.99172, -0.80464)	0.10	432	(-1.05277, -0.35746)
0.20	161	(-0.95988, -0.61285)	106	(-1.01430, -0.85296)	0.20	410	(-1.05955, -0.38317)
		(-0.94584, -0.61636)		(-1.00368, -0.85480)	0.30	389	(-1.06839, -0.43432)
0.40	185	(-0.95313, -0.67034)	113	(-1.02631, -1.05824)	0.40	461	(-1.06595, -0.53404)
		(-0.94548, -0.67168)		(-1.01808, -1.05680)	0.45	331	(-1.03546, -0.62268)
0.495	296	(-0.88715, -0.70783)	138	(-0.90236, -1.30191)	0.495	328	(-0.90548, -0.71043)
		(-0.91352, -0.73436)		(-0.92216, -1.31406)	0.4975	355	(-0.89385, -0.70917)
0.4995	292	(-0.88407, -0.70703)	121	(-0.88160, -1.31135)	0.4995	301	(-0.88520, -0.70694)

Table 1: Reissner-Nordström quasinormal frequency parameter values ( $\rho = -i\omega$ ) for the fundamental ( $n = 0$ ) and two lowest overtones. The quasinormal frequencies appear as complex conjugate pairs in  $\rho$ ; we list only the  $Im(\rho) < 0$  root. The integer listed at the left of each frequency value is the number of terms used by the continued fraction algorithm to obtain a convergence accuracy of 1.2E-09. The third-order WKB values were obtained from reference [22]. Listed are frequencies that correspond to gravitational quadrupole ( $l = 2, i = 2$ ), electric quadrupole ( $l = 2, i = 1$ ), and electric dipole ( $l = 1, i = 1$ ) perturbations at the  $Q = 0$  limit. A double precision version of MINPACK<sup>[39]</sup> routine HYBRD was used for the root search with error tolerance set to 1.0E-05. All computations were done in double precision (53 bit mantissa) FORTRAN on a Sun Microsystems 3/140 computer.

Since expressions (3) – (9) are each real whenever  $\rho$  is real, the Schwartz reflection principle ensures the quasinormal frequencies will appear as complex conjugate pairs in the frequency parameter  $\rho$ . (See references [21] and [22] for further discussion.)

Trajectory plots of the quasinormal frequencies (magnitudes of the real and imaginary parts parameterized by  $Q$ ) are shown in figure 1.

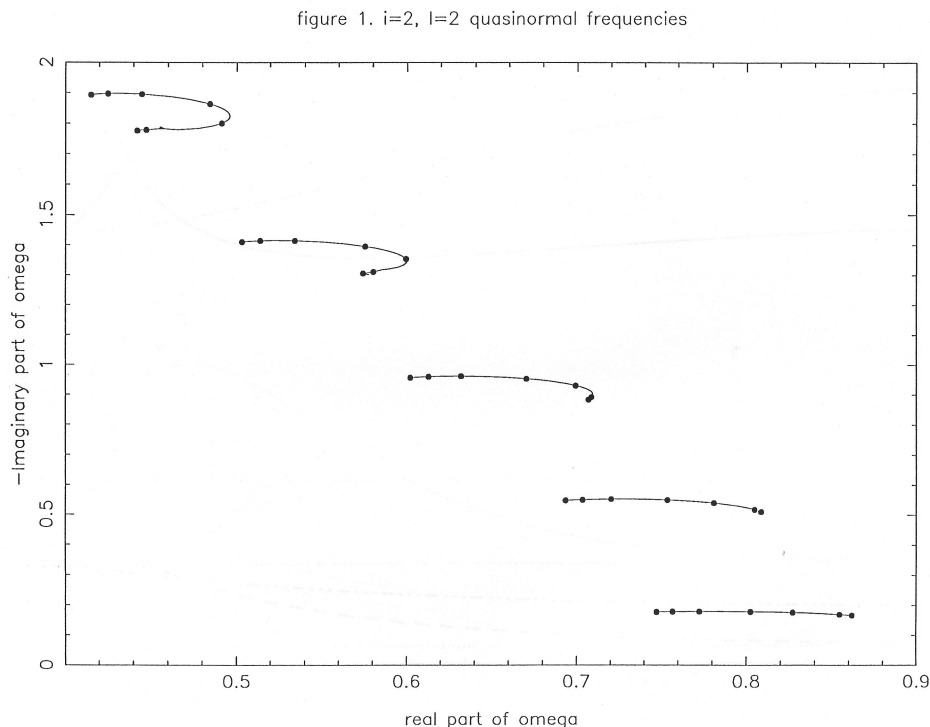


Figure 1: Spacetime diagram of the characteristic-value problem in characteristic  $(u, v)$  coordinates.

Our results confirm that the accuracy of the third order WKBJ quasinormal frequency values tabulated by Kokkotas and Schutz<sup>[22]</sup> can, for a given overtone index, be estimated simply by comparing the WKBJ result with the continued fraction result at the Schwarzschild limit. (Note that Kokkotas and Schutz use a normalization of  $M = 1$ , whereas we have used  $M = 1/2$ .) Agreement between the two methods for the fundamental quadrupole modes is better than a few parts per thousand for  $Q$  less than  $\approx 0.4$ , and becomes only slightly worse for larger  $Q$ . Our continued fraction results agree with the numerical integration results given by Kokkotas and Schutz to within the number of digits supplied for the fundamental mode and at the  $Q = 0$  limit for the higher overtones, but there is mild discrepancy ( $\sim$  few percent) with the numerical results as  $Q$  increases for harmonic index other than zero. In these cases the agreement between the WKBJ and continued fraction results is usually better than the agreement of either with the numerical integration.

## 6 quasinormal mode wavefunctions

The degree to which analytic information appears explicitly factored in representation (3) of the quasinormal mode wavefunction  $Z_i^{(-)}(r)$  can be both useful and deceptive. As an example we observe the behavior of the function as the charge parameter  $Q$  approaches its allowed maximum value  $1/2$ . At maximum  $Q$  the two horizons coalesce to form a confluent singularity in the wave equation, and the tortoise coordinate takes on a somewhat different functional form;  $r_* = r + 2r_c \ln(r - r_c) - r_c^2/(r - r_c)$ , where  $r_c$  is the confluent horizon (an unrealizable naked singularity) located at  $r_c = 1/2$  in our units. As mentioned previously, power series expansions around confluent singular points usually either fail completely or are at best asymptotic. In some cases a judicious choice of Neumann series may be convergent – see reference [28] for an example. There is also no apparent reason why the WKB approximation should not remain valid at maximal  $Q$ , although this has yet to be demonstrated.

Returning to our example, we first factor the identifiably radiative terms from expression (3). Specifically, since  $Re(\rho) < 0$  for quasinormal frequencies, the  $r_+ e^{2\rho r_+} (r_+ - r_-)^{2\rho - 1}$  term in equation (7) becomes infinite as  $Q$ ,  $r_-$ , and  $r_+$  all approach their limiting value  $1/2$ . This could lead to the mistaken conclusion that the transmission coefficient tends uniformly to zero for maximal  $Q$ , which would be at variance both with common sense and with the extensive reflection/transmission coefficient calculations made by Gunter.<sup>[9]</sup> What actually happens is that the increase at large  $r_*$  due to the  $r_+ e^{2\rho r_+} (r_+ - r_-)^{2\rho - 1}$  term is exactly cancelled by a concurrent decrease in the value of the series  $\sum_0^\infty a_n u^n$ . This behavior is illustrated in figures 2 and 3, wherein the complete quasinormal mode wavefunction generated by expression (3) is divided by  $\exp(-\rho|r_*|)$ . Apart from the cusp artifact at  $r_* = 0$  contributed by the denominator, this quotient is quite uniform and the ratio of ingoing (at the horizon) to outgoing (at spatial infinity) flux remains, for these low-lying modes, close to unity for all  $Q$ .

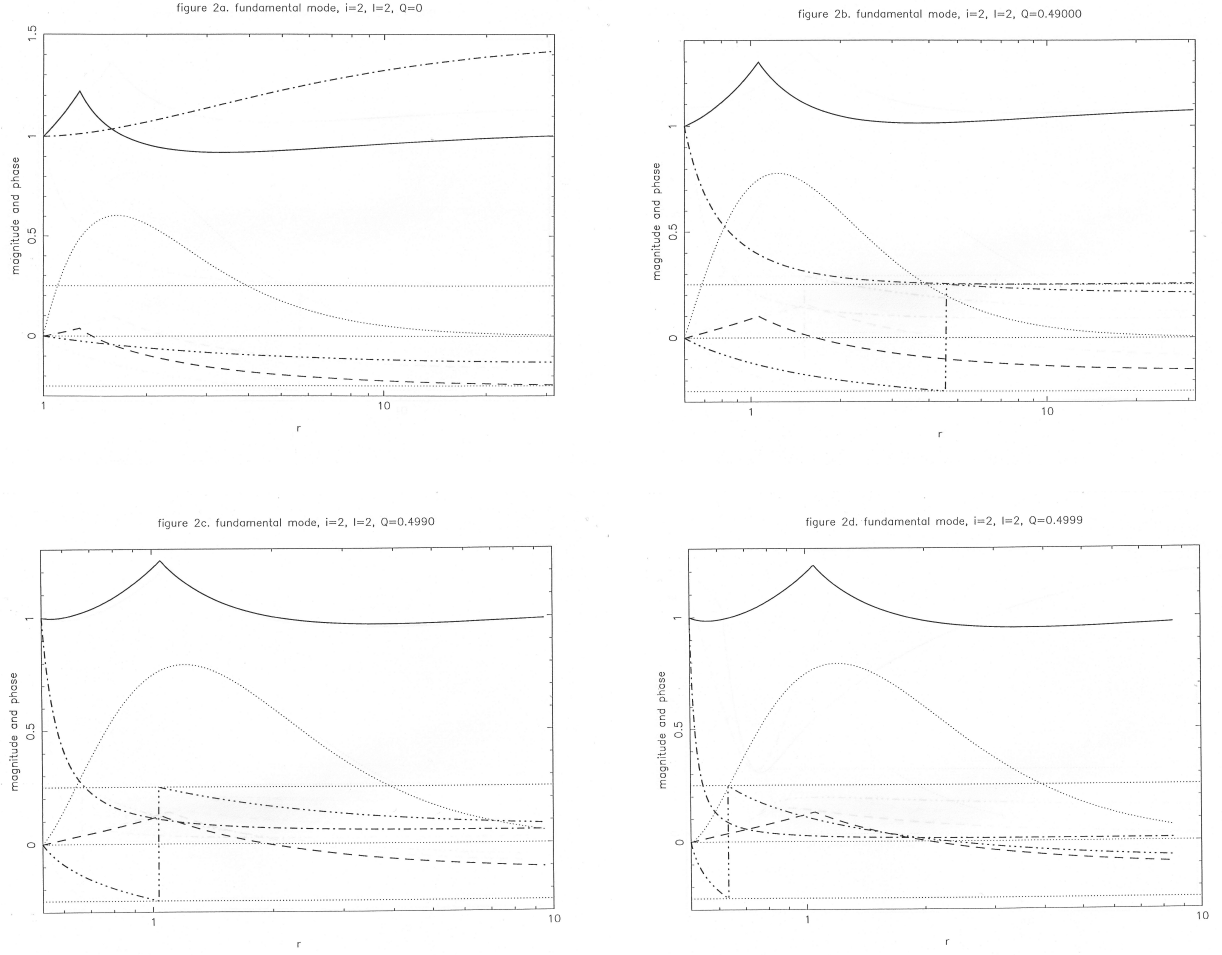


Figure 2: Salient components of the fundamental quadrupole quasinormal mode wavefunction for  $i = 2$  (purely gravitational perturbation at Schwarzschild limit) for different values of  $Q$ : (a)  $Q = 0$  (b)  $Q = 0.4900$  (c)  $Q = 0.4990$  (d)  $Q = 0.4999$ . The solid and dashed lines are the magnitude and phase of expression 3 multiplied by  $\exp(\rho|r_*|)$ . Dash-dot-dash and dash-dot-dot-dot-dash are respectively the magnitude and phase of  $\sum a_n u^n$ . Dotted lines denote the odd-parity potential and the phase limits; the phases have been scaled  $4\pi$  for convenience. The minimum  $r$  value plotted corresponds to the event horizon  $r_+$ .

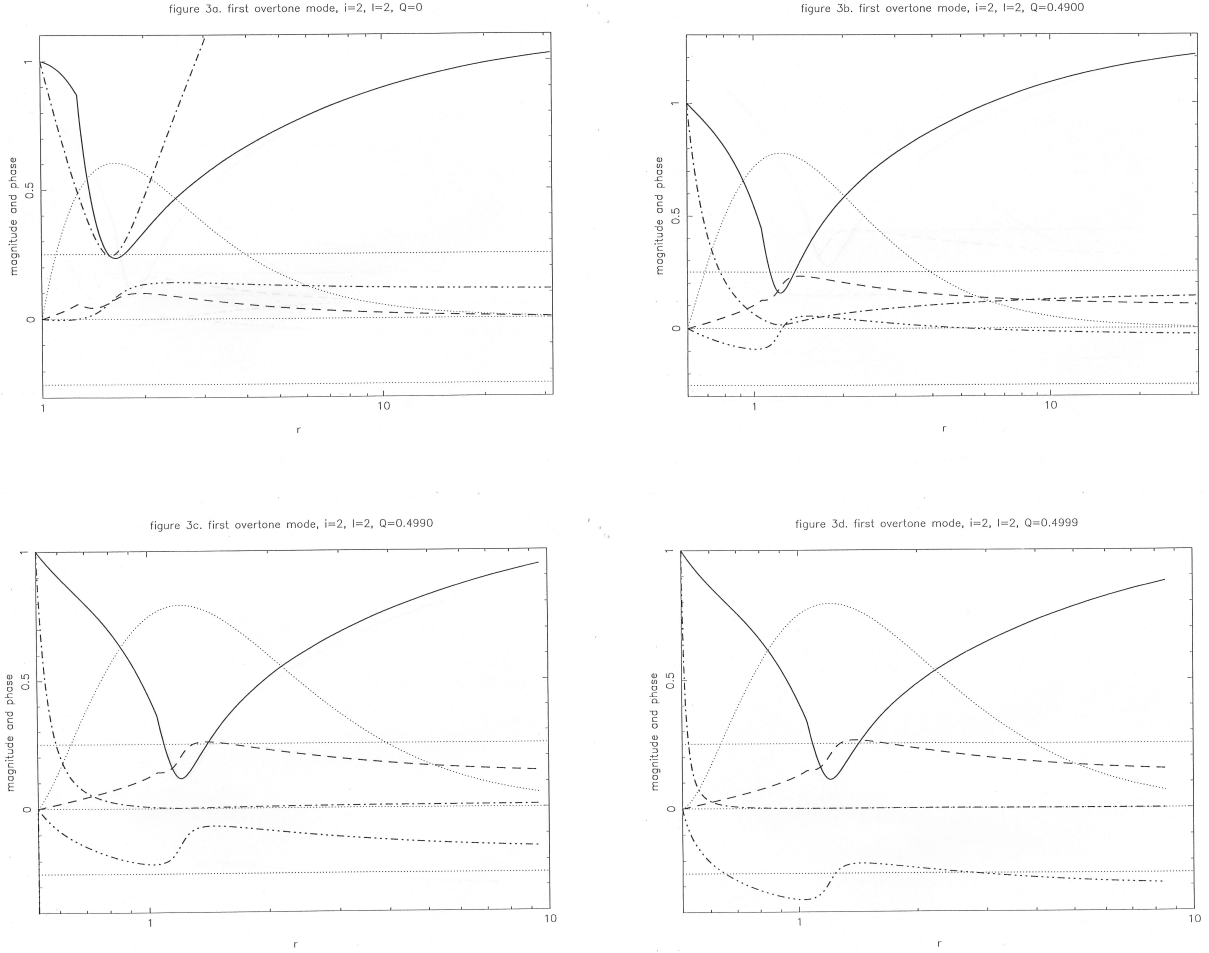


Figure 3: Salient components of the first overtone  $i = 2$  quadrupole quasinormal mode wavefunction. Description of curves same as for Figure 2.

## 7 Conclusion

The algorithms presented here, as are those given previously for Kerr black holes, are straightforward and readily implemented should additional quasinormal frequency values or wavefunctions be desired. As one remark, we did not attempt to track the eighth  $i = 2$  quadrupole overtone (i.e.,  $n = 8$  where  $n = 0$  is the fundamental) as a function of charge. This frequency can be rigorously shown to reduce to the corresponding algebraically special mode's frequency at the Schwarzschild limit,<sup>[46]</sup> but this demonstration and the corresponding relationship between the quasinormal and algebraically special modes (they are *not* the same) is beyond the scope of the present investigation.

We conclude with the following observations: The quasinormal modes of charged black holes, if they are of any astrophysical interest at all, are likely to be so only for holes that are also rapidly rotating. And the master perturbation equations for the Kerr-Newman black hole (chapter 11, equations 145–146 of reference [10]) apparently do not separate. It is likely this non-separability is an unavoidable consequence of Coulomb repulsion destroying the oblate spheroidal symmetry of an uncharged Kerr black hole. But nonseparability need no longer impede the solution of these equations, for the major significance of the present study will be seen to lie, not in its physical

results, but in its demonstration of the validity of matrix determinant methods for solving radiative boundary condition problems typified by the quasinormal ringing of Reissner-Nordström black holes – problems involving banded matrices of order greater than three.

As a result, we feel certain a non-separable eigenfunction expansion can be made for the relevant Kerr-Newman field quantities, and that a spectral or pseudospectral method can be employed for their solution. The key modification to the usual spectral approach will be the introduction of a determinant-zeroing step to enforce boundary conditions and convergence of the series. This approach need not be restricted to the determination of quasinormal frequencies and modes: it could also be applied to expansions in non-separable series of angular functions and Bessel or Coulomb wavefunctions (of adjustable order or phase parameter) in much the same way as was demonstrated for the separable Regge-Wheeler and Generalized Spheroidal wavefunctions in references [16] and [28]. (Such an approach could be termed a pseudospectral Neumann method in the language of reference [47].) The radiative boundary condition at spatial infinity could then be enforced, or the ingoing and outgoing components clearly identified, at any complex frequency for a wide variety of partial differential wave equations. The possible applications of this proposed technique (and some obvious variations) to charged rotating black holes, and to scattering problems in acoustics and electromagnetism, will be subjects of future investigation.

#### Acknowledgements

I thank C.B. Wallace, J.K. Prentice, D.G. Payne and N.H.F. Beebe for useful ideas and discussions. This work was initiated at the BDM Corporation and completed at the Jet Propulsion Laboratory, California Institute of Technology.

## A A proof of equation 22

First consider the three-term recurrence relation that reduces from equations (8) in the Schwarzschild limit when the  $\delta_n$  are zero. We are interested in its behavior for large  $n$ . Scale the recurrence coefficients by  $n^2$  and write them as

$$\begin{aligned}\alpha_n &\sim 1 + u/n \\ \beta_n &\sim -(2 + v/n) \\ \gamma_n &\sim 1 + w/n\end{aligned}\tag{23}$$

where  $u = 2(\rho + 1)$ ,  $v = 8\rho + 2$ , and  $w = 4\rho$ . Divide equation (8) by  $n^2$  and write it as

$$(1 + u/n)\frac{a_{n+1}}{a_n} - (2 + v/n) + (1 + w/n)\frac{a_{n-1}}{a_n} = 0.\tag{24}$$

It is clear that  $\lim_{n \rightarrow \infty} a_{n+1}/a_n = 1$ ; thus more information is needed to establish the convergence of  $\sum_0^\infty a_n$ . Therefore expand the ratio of successive terms in negative powers of  $\sqrt{n}$ ,

$$\frac{a_{n+1}}{a_n} \approx 1 + \frac{a}{\sqrt{n}} + \frac{b}{n} + \dots\tag{25}$$

and substitute back into equation (24):

$$\begin{aligned}&\left(1 + \frac{u}{n}\right) \left(1 + \frac{a}{\sqrt{n}} + \frac{b}{n}\right) - \left(2 + \frac{v}{n}\right) \\ &+ \left(1 + \frac{w}{n}\right) \left(1 - \frac{a}{\sqrt{n}} + \frac{a^2 - b}{n} + \frac{2ab - a/2 - a^3}{n^{3/2}}\right) \approx 0.\end{aligned}\tag{26}$$

Perform the multiplications and retain terms through  $O(n^{-3/2})$ . The coefficient of each power of  $n^{-1/2}$  must vanish independently, hence

$$\begin{aligned}a^2 &= v - u - w &= 2\rho &\text{ and} \\ b &= 1/4 + v/2 - u &= 2\rho - 3/4,\end{aligned}\tag{27}$$

which is the result cited at equation (11).

When  $Q \neq 0$  and the recurrence relation involves four terms, we begin with the reasonable ansatz that the ratios of successive terms  $a_{n+1}/a_n$  will still go to unity at large  $n$ . The ansatz is reasonable because the series  $\sum_0^\infty a_n u^n$  is the solution of a differential equation which has regular singular points at  $u = 0, r_+/r_-$ , and  $-\infty$ , and an irregular singular point at  $u = 1$ . It is reasonable to assume the radius of convergence of such a series solution is exactly one, i.e.,  $\sum_0^\infty a_n u^n$  exists for all  $u$  such that  $|u| \leq 1$ , with equality holding when  $\rho$  is an eigenfrequency. If this is true then equations of the same form as (23-26) *must* hold using the primed coefficients of equations (16) and (17). To see this first let

$$\begin{aligned}\alpha'_n &\sim \kappa(1 + u/n) \\ \beta'_n &\sim -\kappa(2 + v/n) \\ \gamma'_n &\sim \kappa(1 + w/n) .\end{aligned}\tag{28}$$

The constant  $\kappa$  is evaluated by inspecting equation (9):  $\kappa$  must equal  $r_+$  (and  $u = 2b + 2$ ) since  $\alpha'_n = \alpha_n$  for all  $n$ . The remainder of our proof consists of an explicit computation of  $v$  and  $w$ . We

first compute  $\delta_n/\gamma'_{n-1}$ . The denominator is obtained by multiplying the last of equations (28) by  $n^2$ ,

$$\gamma'_n \sim r_+(n^2 + wn) ,$$

from which

$$\gamma'_{n-1} \sim r_+[n^2 + (w-2)n] ,$$

or, dividing again by  $n^2$ ,

$$\gamma'_{n-1} \sim r_+[1 + (w-2)/n] .$$

Retrieve  $\delta_n$  from equation (9),

$$\delta_n \sim r_-[-1 + 2(3 - \rho - b)/n] ,$$

and divide the two to obtain to  $O(1/n)$

$$\frac{\delta_n}{\gamma'_{n-1}} \sim -\frac{r_-}{r_+} \left( 1 + \frac{2\rho + 2b - w - 4}{n} \right) . \quad (29)$$

We substitute this result together with the defining equation (9) for  $\beta_n$  into the third of equations (17) to get

$$\beta'_n = \beta_n - \alpha'_{n-1}\delta_n/\gamma'_{n-1} \quad (30)$$

$$\simeq -r_+\{2n^2 + [2 + 8b - r_-(6b + 2\rho - w)/r_+]n\} , \quad (31)$$

from which we identify  $v$  in terms of  $w$  as

$$v = 2 + 8b - r_-(6b + 2\rho - w)/r_+ . \quad (32)$$

Similarly,

$$\begin{aligned} \gamma'_n &= \gamma_n - \beta'_{n-1}\delta_n/\gamma'_{n-1} \\ &\simeq r_+\{n^2 + [2\rho(1 + 2r_-) + 2b - 4r_-(2b + \rho)/r_+ \\ &\quad + 2r_-^2(3b + \rho)/r_+^2 + w(2r_-/r_+ - r_-^2/r_+^2)]n\} . \end{aligned} \quad (33)$$

The term in square brackets is identified as an explicit expression for  $w$ , which upon simplification yields the desired result,

$$w = 2(\rho + b) , \quad (34)$$

which we can substitute back into (32) to get

$$v = 2 + 4\rho r_+ + 4b . \quad (35)$$

Last, equations (27) give

$$\begin{aligned} a^2 &= v - u - w = 2\rho(r_+ - r_-) \quad \text{and} \\ b &= 1/4 + v/2 - u = 2\rho r_+ - 3/4 , \end{aligned} \quad (36)$$

which reduce to the three-term Schwarzschild result (27) in the limit  $r_- \rightarrow 0$  and  $r_+ \rightarrow 1$ . This completes the proof.

## References

- [1] T. Regge and J.A. Wheeler. *Physical Review*, 108:1063, 1957.
- [2] F.J. Zerilli. *Physical Review D*, 2:2141, 1971.
- [3] Saul A. Teukolsky. Rotating black holes: separable wave equations for gravitational and electromagnetic perturbations. *Physical Review Letters*, 29(16):1114–1117, 1972.
- [4] F.J. Zerilli. *Physical Review D*, 9:860–868, 1974.
- [5] V. Moncreif. *Phys. Rev. D* **9**, 2707 (1974); *ibid.* **10**, 1057 (1975); *ibid.* **12**, 1526 (1975).
- [6] C.V. Vishveshwara. *Nature*, 227:936, 1970.
- [7] S. Chandrasekhar and S. Detweiler. *Proceedings of the Royal Society of London A*, 344:441, 1975.
- [8] Steven Detweiler. In L. Smarr, editor, *Sources of Gravitational Radiation*, page 211. Cambridge University Press, New York, 1979.
- [9] D.L. Gunter. A study of the coupled gravitational and electromagnetic perturbations to the Reissner-Nordström black hole: the scattering matrix, energy conversion, and quasi-normal modes. *Philosophical Transactions of the Royal Society of London A*, 296:497–526, 1980. also *ibid.* **301** 705 (1981).
- [10] S. Chandrasekhar. *The Mathematical Theory of Black Holes*. Clarendon Press, Oxford, 1983.
- [11] L. Dvořák, *Czech. J. Phys. B* **33**, 377–388 (1983); *ibid.* **33**, 510–527 (1983).
- [12] C.V. Vishveshwara. *Physical Review D*, 1:2870, 1970. The poles of the scattering matrix define the quasinormal frequencies: page 2879.
- [13] S. Detweiler. *The Astrophysical Journal*, 239:292, 1980.
- [14] Whether this question was ever really open or not is a matter of opinion. The possibility that there are only a finite number of Schwarzschild quasinormal modes appears to have been suggested by the work of R.H. Price [ *Phys. Rev. D* **5**, 2419–2438 (1972)], who for pedagogical reasons introduced a model potential which had only a finite number of modes (also see reference [7]). In the same paper however, Price also gave strong arguments that his model potential would not accurately reflect the properties of the actual black hole potential in this respect, and predicted an infinite number of Schwarzschild quasinormal frequencies. Although one can show that any small deformation of Price’s potential also produces an infinity of quasinormal frequencies, ideally one would like a closed-form asymptotic expression for Schwarzschild quasinormal frequencies that, in the limit of very high damping, agrees with the continued fraction results.
- [15] E.W. Leaver. An analytic representation for the quasinormal modes of Kerr black holes. *Proceedings of the Royal Society of London A.*, 402:285–298, 1985.
- [16] E.W. Leaver. Spectral decomposition of the perturbation response of the Schwarzschild geometry. *Physical Review D.*, 34:384–408, 1986.

- [17] B. Mashhoon in *Proceedings of the Third Marcel Grossman Meeting on Recent Developments of General Relativity Shanghai, 1982* (Hu Ning, editor). North-Holland, Amsterdam, (1983); also *Mitt. Astron. Ges.* **58**, 164 (1983).
- [18] Bernard F. Schutz and Clifford M. Will. Black hole normal modes: A semianalytic approach. *The Astrophysical Journal*, 291:L33–L36, 1985.
- [19] Hans-Joachim Blome and Bahram Mashhoon. Quasi-normal oscillations of a schwarzschild black hole. *Physics Letters*, 100A:231, 1984.
- [20] Sai Iyer and Clifford M. Will. Black-hole normal modes: a WKBJ approach. i. foundations and application of a higher WKBJ analysis of potential barrier scattering. *Physical Review D*, 35:3621, 1987.
- [21] V. Ferrari and B. Mashhoon. *Physical Review D*, 30:295, 1984.
- [22] Kostas D. Kokkotas and Bernard F. Schutz. Black hole normal modes, a WKBJ approach. iii. the Reissner-Nordström black hole. *Physical Review D*, 37:3378, 1988.
- [23] Lucy Joan Slater. Confluent hypergeometric functions. In Milton Abramowitz and Iren A. Stegun, editors, *Handbook of Mathematical Functions*, pages 331–354. National Bureau of Standards, 1964.
- [24] In the case of black holes the coordinate singularities correspond to the center of the Schwarzschild hole and its horizon, or to the inner and outer horizons of the Kerr black hole.
- [25] A.H. Wilson. A generalized spheroidal wave equation. *Proceedings of the Royal Society of London A.*, 118:617–635, 1928.
- [26] J.A. Stratton, P.M. Morse, L.J. Chu, J.D.C. Little, and F.J. Corbatto. *Spheroidal Wavefunctions*. John Wiley and Sons, New York, 1956.
- [27] Arnold N. Lowan. Spheroidal wavefunctions. In Milton Abramowitz and Irene A. Stegun, editors, *Handbook of Mathematical Functions*, pages 751–770. National Bureau of Standards, 1964.
- [28] E.W. Leaver. Solutions to a generalized spheroidal wave equation: Teukolsky’s equations in general relativity, and the two-center problem in molecular quantum mechanics. *Journal of Mathematical Physics*, 27:1238–1265, 1986.
- [29] R.F. Arenstorf, J.M. Cohen, and L.S. Kegeles, *J. Math. Phys.* **19**, 833-837 (1978); M.W. Kearney, L.S. Kegeles, and J.M. Cohen, *Astrophysics and Space Science* **56**, 129–190, (1978).
- [30] S. Persides, *J. Math. Phys.* **14**, 1017–1021 (1972); *Comm. Math. Phys.* **48**, 165–189 (1976); *ibid.* **50**, 229–239 (1976).
- [31] F.M. Arscott, P.J. Taylor, and R.V.M. Zahar. On the numeric construction of ellipsoidal wavefunctions. *Mathematics of Computation*, 40:367–380, 1983.
- [32] S. Chandrasekhar. *Proceedings of the Royal Society of London A.*, 369:425, 1980.

- [33] See reference ([10]), page 237.
- [34] G. Jaffé. *Zeitschrift für Physik*, 87:535, 1934.
- [35] W.G. Baber and H.R. Hassé. The two centre problem in wave mechanics. *Proceedings of the Cambridge Philosophical Society*, 25:564–581, 1935.
- [36] Mikio Shimizu. Two center coulomb approximation. *Journal of the Physical Society of Japan*, 18(6):811–819, 1963.
- [37] As was initially shown for Hydrogen molecule-like ions by E. Hylleraas,<sup>[48]</sup> G. Jaffe,<sup>[34]</sup> and W. Baber and H. Hassé.<sup>[35]</sup>
- [38] J.J. Dongarra, C.B. Moler, J.R. Bunch, and G.W. Stewart. *Linpac User's Guide*. SIAM, Philadelphia, 1979. Both the Linpack and Minpack libraries are public domain and are frequently distributed as part of other mathematical software packages (individual routines are occasionally renamed).
- [39] Jorge J. Moré, Burton S. Garbow, and Kenneth E. Hillstom. *User's Guide for MINPACK-1*. Argonne National Laboratory, National Technical Information Service, U.S. Department of Commerce, 5285 Port Royal Road, Springfield, VA 22161, 1980.
- [40] W. Gautschi. Computational aspects of three-term recurrence relations. *SIAM Review*, 9:24–82, 1967.
- [41] There are several algorithms for propagating three-term recurrence series, and they have slightly different numerical properties when implemented in finite precision arithmetic. We prefer J.C.P. Miller's algorithm.<sup>[40]</sup>
- [42] See appendix A of reference [16].
- [43] We have previously referred to this continued fraction algorithm as “Steed's Algorithm” (c.f. reference [49]). Steed's is apparently an independent derivation of a formulation given by equations (1.9) and (1.10) of reference [40], wherein its origins are traced to still earlier work by Teichrow<sup>[50]</sup> and Wall<sup>[51]</sup>.
- [44] See reference ([25]) and the citations therein.
- [45] For the  $q^{\text{th}}$  overtone frequency  $\rho_q$  approximately the first  $q$  components of the solution vector  $\{a_n\}$  actually increase in magnitude according to the upper sign in (12) before convergence sets in according to the lower: approximately  $q$  inversions of the continued fraction (19) provide the most stable function for the root search.
- [46] B.F. Whiting and E.W. Leaver, unpublished result.
- [47] David Gottlieb, M. Yousuff Hussaini, and Steven A. Orzag. Spectral methods for partial differential equations. chapter Theory and Applications of Spectral Methods. SIAM, Philadelphia, 1984.
- [48] Egil Hylleraas. *Zeitschrift für Physik*, 71:739, 1931.
- [49] A.R. Barnett, D.H. Feng, J.W. Steed, and L.J.B. Goldfarb. Coulomb wavefunctions for all real  $\eta$  and  $\rho$ . *Computer Physics Communications*, 8:377, 1974.

- [50] D. Teichroew. Use of continued fractions in high speed computing. *Math. Tables Aids Comput.*, 6:127–133, 1952.
- [51] H.S. Wall. *Analytic Theory of Continued Fractions*. D. van Nostrand, New York, 1948.

## Figure and Table captions

**table 1: caption:** Reissner-Nordström quasinormal frequency parameter values

( $\rho = -i\omega$ ) for the fundamental ( $n = 0$ ) and two lowest overtones. The quasinormal frequencies appear as complex conjugate pairs in  $\rho$ ; we list only the  $Im(\rho) < 0$  root. The integer listed at the left of each frequency value is the number of terms used by the continued fraction algorithm to obtain a convergence accuracy of 1.2E-09. The third-order WKBJ values were obtained from reference [22]. Listed are frequencies that correspond to gravitational quadrupole ( $l = 2, i = 2$ ), electric quadrupole ( $l = 2, i = 1$ ), and electric dipole ( $l = 1, i = 1$ ) perturbations at the  $Q = 0$  limit. A double precision version of MINPACK<sup>[39]</sup> routine HYBRD was used for the root search with error tolerance set to 1.0E-05. All computations were done in double precision (53 bit mantissa) FORTRAN on a Sun Microsystems 3/140 computer.

**figure 1: title:** Quasinormal frequencies for  $l=2, i=2$ .

**x-axis:**  $Re(\omega)$

**y-axis:**  $-Im(\omega)$

**caption:** Quasinormal frequency trajectories for the  $i=2$  quadrupole mode parameterized by the charge  $Q$ . Fundamental mode appears at lower right, fourth overtone at upper left. Tick marks (from right to left) correspond to  $Q = 0, 0.2, 0.3, 0.4, 0.45, 0.49$ , and  $0.499$ .

**figure 2: title:** Figure 2. fundamental  $i = 2$  quadrupole mode for increasing values of  $Q$ .

**x-axis:**  $r$

**y-axis:** magnitude and phase

**caption:** Salient components of the fundamental quadrupole quasinormal mode wavefunction for  $i = 2$  (purely gravitational perturbation at Schwarzschild limit) for different values of  $Q$ : (a)  $Q = 0$  (b)  $Q = 0.4900$  (c)  $Q = 0.4990$  (d)  $Q = 0.4999$ . The solid and dashed lines are the magnitude and phase of expression 3 multiplied by  $\exp(\rho|r_*|)$ . Dash-dot-dash and dash-dot-dot-dot-dash are respectively the magnitude and phase of  $\sum a_n u^n$ . Dotted lines denote the odd-parity potential and the phase limits; the phases have been scaled  $4\pi$  for convenience. The minimum  $r$  value plotted corresponds to the event horizon  $r_+$ .

**figure 3: title:** Figure 3. first overtone  $i = 2$  quadrupole mode for increasing values of  $Q$ .

**x-axis:**  $r$

**y-axis:** magnitude and phase

**caption:** Salient components of the first overtone  $i = 2$  quadrupole quasinormal mode wavefunction. Description of curves same as for Figure 2.

Table 1.

Q	$l = 2, i = 2$		$l = 2, i = 1$		Q	$l = 1, i = 1$	
n=0							
0.00	45	(-0.17792, -0.74734)	39	(-0.19001, -0.91519)	0.00	74	(-0.18498, -0.49653)
wkbj		(-0.17844, -0.74632)		(-0.19012, -0.91426)	0.10	75	(-0.18580, -0.50295)
0.20	48	(-0.17880, -0.75687)	41	(-0.19288, -0.95985)	0.20	76	(-0.18831, -0.52384)
		(-0.17928, -0.75584)		(-0.19296, -0.95896)	0.30	80	(-0.19241, -0.56551)
0.40	63	(-0.17929, -0.80243)	48	(-0.19814, -1.14026)	0.40	93	(-0.19654, -0.64699)
		(-0.17968, -0.80108)		(-0.19798, -1.13952)	0.45	98	(-0.19487, -0.72165)
0.495	146	(-0.16853, -0.85859)	92	(-0.17728, -1.38550)	0.495	150	(-0.17420, -0.84279)
		(-0.17064, -0.85660)		(-0.17834, -1.38500)	0.4975	174	(-0.17086, -0.85253)
0.4995	244	(-0.16708, -0.86227)	145	(-0.17255, -1.40620)	0.4995	228	(-0.16776, -0.86062)
0.49995	313	(-0.16729, -0.86196)	149	(-0.17241, -1.40815)	0.49995	218	(-0.16686, -0.86283)
n=1							
0.00	81	(-0.54783, -0.69342)	63	(-0.58142, -0.87308)	0.00	181	(-0.58733, -0.42903)
wkbj		(-0.54982, -0.69204)		(-0.58194, -0.87166)	0.10	176	(-0.58935, -0.43626)
0.20	84	(-0.55025, -0.70346)	65	(-0.58938, -0.92000)	0.20	175	(-0.59533, -0.45977)
		(-0.55218, -0.70196)		(-0.58968, -0.91856)	0.30	181	(-0.60450, -0.50661)
0.40	106	(-0.54989, -0.75381)	75	(-0.60212, -1.10999)	0.40	198	(-0.61070, -0.59802)
		(-0.55250, -0.75096)		(-0.60136, -1.10812)	0.45	180	(-0.59979, -0.68087)
0.495	197	(-0.51403, -0.80704)	111	(-0.53501, -1.35732)	0.495	220	(-0.52932, -0.79794)
		(-0.52868, -0.80676)		(-0.54230, -1.35788)	0.4975	241	(-0.52000, -0.80390)
0.4995	257	(-0.51030, -0.80875)	136	(-0.52144, -1.37419)	0.4995	260	(-0.51197, -0.80812)
0.49995	190	(-0.51411, -0.78618)	104	(-0.52512, -1.36630)	0.49995	98	(-0.51941, -0.81204)
n=2							
0.00	154	(-0.95655, -0.60211)	105	(-1.00318, -0.80237)	0.00	446	(-1.05038, -0.34955)
wkbj		(-0.94212, -0.60586)		(-0.99172, -0.80464)	0.10	432	(-1.05277, -0.35746)
0.20	161	(-0.95988, -0.61285)	106	(-1.01430, -0.85296)	0.20	410	(-1.05955, -0.38317)
		(-0.94584, -0.61636)		(-1.00368, -0.85480)	0.30	389	(-1.06839, -0.43432)
0.40	185	(-0.95313, -0.67034)	113	(-1.02631, -1.05824)	0.40	461	(-1.06595, -0.53404)
		(-0.94548, -0.67168)		(-1.01808, -1.05680)	0.45	331	(-1.03546, -0.62268)
0.495	296	(-0.88715, -0.70783)	138	(-0.90236, -1.30191)	0.495	328	(-0.90548, -0.71043)
		(-0.91352, -0.73436)		(-0.92216, -1.31406)	0.4975	355	(-0.89385, -0.70917)
0.4995	292	(-0.88407, -0.70703)	121	(-0.88160, -1.31135)	0.4995	301	(-0.88520, -0.70694)